Transportation Research Part C 95 (2018) 582–598

Contents lists available at ScienceDirect

Transportation Research Part C

journal homepage: www.elsevier.com/locate/trc

Vehicle actuated signal performance under general traffic at an isolated intersection

Xiubin Bruce Wang[a,*], Kai Yin[b], Henry Liu[c]

[a] Zachry Department of Civil Engineering, Texas A & M University, College Station, TX 77843, United States
[b] HomeAway, Austin, TX 78727, United States
[c] Department of Civil and Environmental Engineering, University of Michigan, Ann Arbor, MI 48109, United States

ARTICLE INFO

Keywords:
Actuated signal control
Vehicle delay
Traffic control
Queuing system

ABSTRACT

We study green extension of a two-phased vehicle actuated signal at an isolated intersection between two one-way streets. The green phase is extended by a preset time interval, referred to as critical gap, from the time of a vehicle actuation at an advance detector. The green phase switches if there is no arrival during the critical gap. We develop an exact model to study the intersection performance with traffic following Poisson processes. We further extend the model to approximate the case of general traffic. Our model in the general case works well compared with Monte Carlo simulation. A few major observations include: (1) The optimal critical gap decreases with the traffic; (2) The optimal critical gap can be much larger (up to 5 s) than the common presumption of 2–3 s; (3) Queue clearance policy is not nearly optimal in general even in the case of heavy traffic.

1. Introduction

Vehicle actuated signal systems have been widely adopted in traffic control at road intersections for their adaptability to traffic. Among the over 150,000 signalized intersections in the major 106 metropolitan areas surveyed in 2004 by the Bureau of Transportation Statistics, over 50 percent are fully or semi actuated (FHWA, 2004). This percentage indicates a stunning number of actuated intersections nation or world wide, not considering the increasing percentage of actuated intersections due to deployment of intelligent transportation systems (ITS). It is therefore significant to study control strategies at these intersections in order to alleviate the exacerbating urban traffic congestion.

A current consensus among various signal control schemes is that green time should first guarantee queue clearance at each direction. A major difference between them is in how to extend the green time after the vehicle queue has been dissipated. In this paper, we study a special scheme that controls the green extension solely based on the time interval between vehicle arrivals (referred to as headway or gap for simplicity) after queued vehicles have been discharged. In this scheme, typically an advance detector is located at a distance prior to the intersection such that an arriving vehicle triggers a green time extension in order to pass through without stop. This extended time period actuated by the vehicle is called *critical gap* in this paper. If there is no vehicle actuation during a critical gap, the green phase switches to clear queues in other approaches. In this way, the actuated system dynamically allocates the green time between multiple approaches according to vehicle arrivals. Note that the terms gap and headway are exchangeable in this paper and are both measured in time.

Clearly, the critical gap is the control variable in this special scheme. Configuration of the critical gap in such a scheme is

* Corresponding author.
E-mail address: bwang@tamu.edu (X.B. Wang).

https://doi.org/10.1016/j.trc.2018.08.002
Received 22 December 2017; Received in revised form 18 June 2018; Accepted 4 August 2018

important to the overall signal performance as it determines the total green duration in each approach. In addition, the green durations of approaches have a profound effect on each other. Take an intersection between two one-way streets, namely approach 1 and approach 2, as an example. A green duration of approach 1 largely determines the number of waiting vehicles accumulated in approach 2, and has impact on the immediate next green duration of approach 2. Similarly, the green duration of approach 2 impacts that of approach 1. In this way, the characteristics in both approaches interact to determine the signal evolution and intersection performance. Therefore, the critical gap in one approach, although seemingly only affects directly the green duration of its own approach, has implications to all the green phases.

In this paper, through an idealized intersection between two one-way streets, we examine the signal system performance in relation to the setup of critical gaps. The purpose of the paper is not to provide a tool for general intersection performance evaluation, but for insights into this complex control scheme through simple cases. Literature has indicated that even a reasonably sized intersection with moderate traffic is difficult to model.

Many literature and practices assume that the critical gap is exogenous, and that it is determined by the travel time from an upstream loop detector to the intersection (see, for example, Bonneson and Mccoy, 1995). This paper, instead, coincides with several pioneer works such as Darroch et al. (1964), Newell (1969), Cowan (1978), and later Viti and Van Zuylen (2010), which all take the critical gap endogenous. We will analytically examine its effect on intersection performance in this paper. The findings about critical gap will help determine the location of detectors prior to intersections.

The significance of the critical gap to the signal performance at an actuated intersection has long been recognized (for examples, Akçelik, 1981; Lin, 1982a; Courage et al., 1996). A major implication as mentioned earlier, the critical gap largely determines the dynamic interaction of phases by directly affecting the random green times. It is a challenging task to consider the interactive random phases for intersection signal performance. There are two classes of literature according to how the random phases are treated in modeling. In the first class, models represent each random phase with its expected green time duration. Some representative literature of this class includes Akçelik (1994), Lin (1982b) and Lin and Courage (1996). When the random green times are represented by their expected values, resemblance of the 'system' to the fixed timing signal gives rise to many formulas following the format of the Webster's equation (Webster, 1958) such as Kimber and Hollis (1979) and Akçelik (1994). An advantage of models in this class is its relative simplicity for modeling and (often) empirical formulas for easy application. The well-known works along this line include Akçelik and Rouphail (1993), Akçelik et al. (1997), Daniel et al. (1996), Li et al. (1994, 1996), Malakapalli and Messer (1993), and Rouphail et al. (1997). Our work falls in the second class of literature such as Darroch et al. (1964), Newell (1969), and Cowan (1978), which models phase interaction by explicitly considering each phase as a random variable. The second class of literature is rather scant, primarily because of the inherent technical challenges and rather restrictive assumptions.

Darroch et al. (1964) and Tanner (1953) appear to be the only two developing exact analytical models in settings very similar to ours. Both of them develop analytical models to this complex traffic control problem, but neither conducted numerical tests probably due to the then limited computing power. There are some other literature, as mentioned in Darroch et al. (1964), each studying a similar problem in a different but rather restrictive setting. For example, Hawkes (1963) studies the performance with zero green extension and zero time loss from switching. Lehoczky (1972) studies the bunching effect of vehicle arrivals. In the 1970s, additional research was conducted. Cowan (1978) studies bunch arrivals but assumes a vehicle headway within bunches. Cowan (1978) specially treats vehicle headway greater than a value 1.0, which is unnecessary because headway can be any nonnegative value when multiple lanes are considered in a direction. After the 1980s, there has been little analytical result on this problem except for a few examples such as Mirchandani and Ning (2007) and Viti and Van Zuylen (2010). The intersection control is a complex process. The early attempts to modeling this process are rather limited.

In this paper, we study two scenarios, Poisson processes of vehicle arrivals and general stationary arrivals of heavy traffic respectively, both of which trace back to their origins of literature as early as in the 1950s. The first scenario addresses a similar problem as in Darroch et al. (1964), but with a different modeling methodology and more extensive numerical tests. A primary contribution of this paper is made in the second scenario with stationary and heavy traffic, which has never been studied before in our best knowledge. The first scenario sets the framework for the second to build on. In the second scenario, we develop asymptotic models in general traffic taking green extension as endogenous. Our developed formulas evaluate the intersection performance well, assessed with numerical simulation, when the critical gap is present. Among the relevant literature, Newell (1969) develops approximated performance evaluation in a restrictive condition that does not allow green extension.

Organization of this paper is as follows. In Section 2, we define the problem, followed by development of analytical formulas for the expected green times, their variances as well as vehicle delay. Section 3 develops delay function in terms of green extension. Section 4 extends the study into the case of stationary and heavy traffic. We conclude this paper in Section 5.

2. Expectation and variance of green times

We start with the problem definition between two one-way streets.

2.1. Problem statement

Consider a fully actuated signal system at an isolated intersection between two one-way streets without turning vehicles, characterized by a major and a minor approaches respectively. We assume that there are only two phases, each dedicated to traffic in one approach. Each phase has a green and a red time intervals. Vehicles proceed in green and stop in red signals. Vehicle arrivals from the two approaches follow two homogeneous Poisson processes. We consider a special yet popular control scheme whose green interval

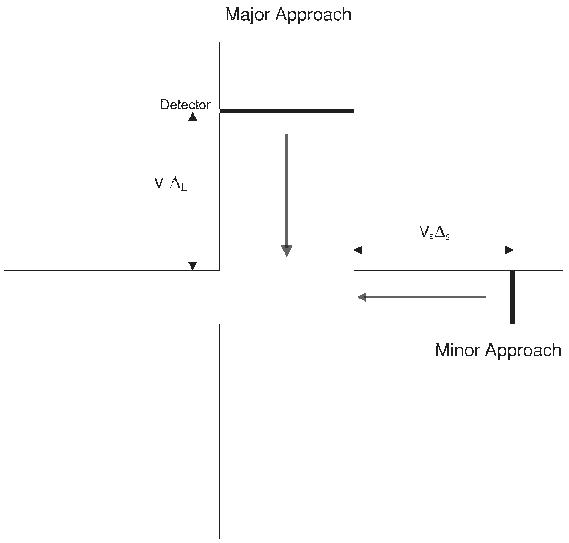

Fig. 1. A major-minor intersection.

first ensures queue clearance and whose green extension after queue clearance is controlled by a vehicle detector placed upstream of each incoming approach. Under a green signal, a vehicle passage by the detector at time t triggers the green extended until time $t + \Delta$ or until queued vehicles are cleared, whichever is later. Δ is called *critical gap* to allow an arriving vehicle to pass through the intersection without a stop. It is usually the travel time from the vehicle detector to the intersection stop line. If no vehicle arrival triggers further green extension, the green signal phases out and switches to its conflict approach automatically, resulting in a loss δ_i, $i \in \{s, L\}$, of effective green time. Here $\delta = \delta_s + \delta_L$. The critical gaps are denoted by Δ_s and Δ_L for the minor and major approaches, respectively. Obviously, the critical gaps Δ_s and Δ_L are the only control variables. The objective is to decide the values of Δ_s and Δ_L such that the average vehicle delay at the intersection over a long period is minimized.

To summarize a cycle process briefly, a signal cycle goes with a green time t_L for the major approach, followed by an All-Red interval δ_s, and sequentially followed by a green interval t_s for the minor approach before another All-Red interval δ_L, where $\delta = \delta_s + \delta_L$. The cycle repeats itself onwards.

Fig. 1 illustrates such an intersection and Fig. 2 shows an example of green extension in one cycle. In the case of multi-lanes, an equivalent one lane case is obtained by projecting vehicles onto one lane, which justifies the point assumption of vehicles as in Darroch et al. (1964). Similar problem setups are also seen in Tanner (1953), Darroch et al. (1964), Newell (1969), Cowan (1978), in which the critical gap is the only control variable.

In Sections 2 and 3, we develop models addressing traffic of Poisson processes. In Section 4, we only require the traffic to be heavy and follow a stationary process with an i.i.d. headway.

Note that loop detectors are usually at a distance, $v_s\Delta_s$ and $v_L\Delta_L$, before the intersection for both incoming approaches respectively, where v_s and v_L are the respective average speeds for both roads. We do not consider minimum green time and maximum green time, a similar treatment as in Darroch et al. (1964). This implies a reasonable assumption that technologies are available to detect vehicle queue presence. This setup allows us to explore for the full potential of efficient signal control. Note again that this paper does

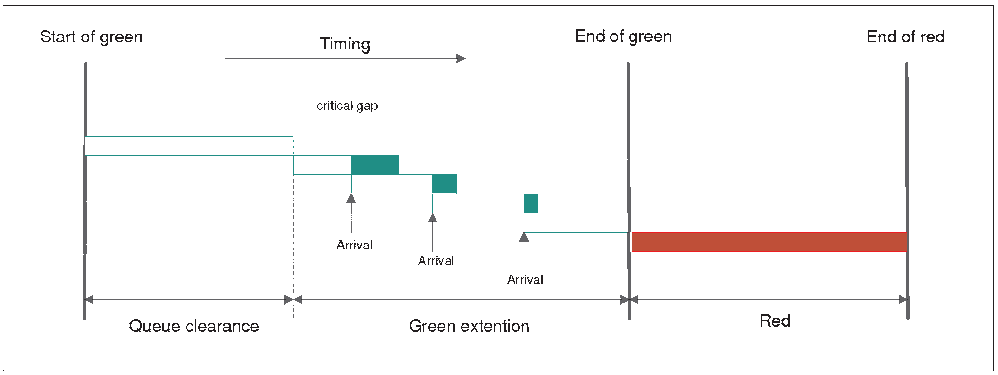

Fig. 2. A process of green extension for one phase (time goes from left to right). (For interpretation of the references to color in this figure legend, the reader is referred to the web version of this article.)

not concern practical implementations, but the maximum potential of intersection control. We believe the findings directly shed light on practices.

Strategy

To briefly summarize, we assume a *strategy* in which the green phase always switches to its conflict approach when there is no vehicle arrival during the period of the most recently extended critical gap. This assumption is critical to modeling as argued in Darroch et al. (1964). In contrary, Tanner (1953) considers a strategy not switching signal if no vehicle arrives in the conflict direction, meeting insurmountable technical difficulties for modeling.

We refer to our strategy as the *always-switch* strategy. Although the *always-switch* strategy could give rise to a 'peculiar' situation under light traffic in which the currently green phase switches to the minor approach without any waiting vehicles, and then switches back to the major approach, there is a high probability of vehicle presence at the time of switch in heavy traffic. Therefore, Darroch et al. (1964) argue that models under this strategy make good approximation to the actual performance.

As will be seen, vehicle delay and green times are functions of the total switching loss of green time in a cycle, irrespective of the loss time split between switches. δ represents the total time loss for the two switches during a signal cycle.

We present the notations next, where the subscripts s and L correspond to the minor and major approaches, respectively.

Notation	
λ_s	vehicle arrival rate along the minor approach
λ_L	vehicle arrival rate along the major approach
Δ_s	critical gap in the minor approach
Δ_L	critical gap in the major approach
t_s	random green time in the minor approach
t_L	random green time in the major approach
f_s	discharge rate of vehicular queue along the minor approach
f_L	discharge rate of vehicular queue along the major approach
δ	total green time loss in a signal cycle due to phase switches
$E[\cdot]$	expected value function
$Var(\cdot)$	variance function
$X(\cdot)$	random number of arrivals in the minor approach in a time period
D_s, D_L	constant discharge headway for the minor and major directions respectively, where $D_s = \frac{1}{f_s}$ and $D_L = \frac{1}{f_L}$

The parameters of the intersection, such as the green time loss and queue discharge rates, are all deterministic here. We believe that assuming randomness for them would only increase technical complexity slightly and that it would not change the nature of the findings. In addition, the critical gaps, once set up, do not change during a control process.

We first examine the expected duration of green intervals for both approaches. These expected values will be used throughout this paper.

2.2. Expected green times

In each approach, the green interval consists of two random components: queue clearance time and free flow time. The queue clearance time represents the period in which the discharge rate of vehicles equals the saturation rate, denoted by t_{sa} and t_{La} for both approaches, respectively. The free flow time, denoted by t_{sb} and t_{Lb} for both approaches respectively, corresponds to the period of time when incoming vehicles pass the intersection without a stop, the length of which is a function of the critical gap and vehicle arrivals. In the free flow time, there is no presence of vehicular queue. The critical gap is the endogenous variable to be studied. As a special case, if the critical gap is set to be zero, which means the signal switches immediately after queue clearance, - a queue clearance policy, the free flow time becomes zero.

As studied in Wang (2007), t_{sb} and t_{Lb} are determined by an information relay process: $E[t_{sb}] = \frac{1}{\lambda_s}e^{\lambda_s\Delta_s} - \frac{1}{\lambda_s} - \Delta_s$, and $E[t_{Lb}] = \frac{1}{\lambda_L}e^{\lambda_L\Delta_L} - \frac{1}{\lambda_L} - \Delta_L$. Note that similar formulas are also available in Akçelik (1994) and Lin (1982b). In addition, we have $t_s = t_{sa} + t_{sb}$ and $t_L = t_{La} + t_{Lb}$. Due to the Markov property, t_{sa} and t_{sb} are independent of each other. The same is true for t_{La} and t_{Lb}. Fig. 3 is an illustrative queuing process in the minor direction during a cycle.

Next, we show how to evaluate t_{sa}. t_{sa} satisfies the following relationship for traffic flow conservation.

$$X(t_L + \delta - \Delta_s) + X(t_{sa}) - f_s t_{sa} = 0, \tag{1}$$

where $X(\cdot)$ represents the number of arrivals in a Poisson process along the minor approach. Eq. (1) states that the total number of vehicles discharged at the saturation rate in time t_{sa} equals to the total arrivals during $t_L + \delta + t_{sa} - \Delta_s$. Here Δ_s is a proven time interval in which no vehicles arrive at the intersection owing to the upstream vehicle detectors. Eq. (1) ensures a full discharge rate during t_{sa}.

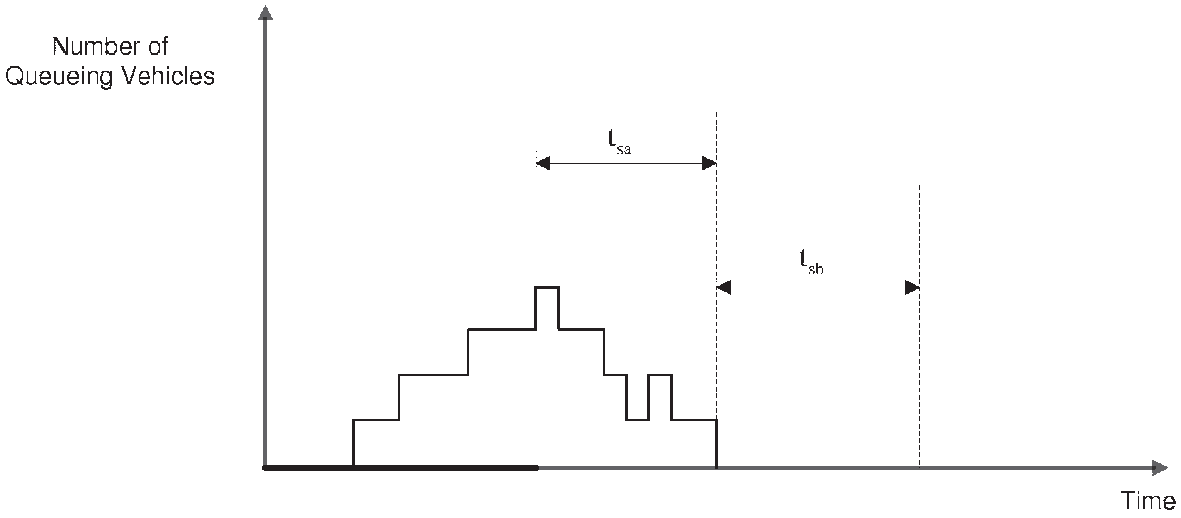

Fig. 3. An illustrative queuing process in the minor direction.

Taking expectation at both sides of Eq. (1) gives the following expected queue clearance time.

$$E[t_{sa}] = \frac{\lambda_s E[t_L] + \lambda_s \delta - \lambda_s \Delta_s}{f_s - \lambda_s}.$$

Similarly,

$$E[t_{La}] = \frac{\lambda_L E[t_s] + \lambda_L \delta - \lambda_L \Delta_L}{f_L - \lambda_L}.$$

We have

$$E[t_s] = E[t_{sa}] + E[t_{sb}] = \frac{\lambda_s E[t_L] + \lambda_s \delta}{f_s - \lambda_s} + \frac{1}{\lambda_s} e^{\lambda_s \Delta_s} - \frac{1}{\lambda_s} - \frac{f_s}{f_s - \lambda_s} \Delta_s. \tag{2}$$

In the same way,

$$E[t_L] = \frac{\lambda_L E[t_s] + \lambda_L \delta}{f_L - \lambda_L} + \frac{1}{\lambda_L} e^{\lambda_L \Delta_L} - \frac{1}{\lambda_L} - \frac{f_L}{f_L - \lambda_L} \Delta_L. \tag{3}$$

Solving (2) and (3) gives $E[t_s]$ and $E[t_L]$ as follows.

Proposition 1. *The expected lengths of green phases are given as follows.*

$$E[t_s] = \frac{(f_s - \lambda_s)(f_L - \lambda_L)}{f_s f_L - f_s \lambda_L - f_L \lambda_s} \times \left\{ \frac{\lambda_s \delta}{f_s - \lambda_s} + \frac{1}{\lambda_s} e^{\lambda_s \Delta_s} - \frac{1}{\lambda_s} - \frac{f_s}{f_s - \lambda_s} \Delta_s + \frac{\lambda_s}{f_s - \lambda_s} \left(\frac{\lambda_L \delta}{f_L - \lambda_L} + \frac{1}{\lambda_L} e^{\lambda_L \Delta_L} - \frac{1}{\lambda_L} - \frac{f_L}{f_L - \lambda_L} \Delta_L \right) \right\}, \tag{4}$$

and

$$E[t_L] = \frac{(f_s - \lambda_s)(f_L - \lambda_L)}{f_s f_L - f_s \lambda_L - f_L \lambda_s} \times \left\{ \frac{\lambda_L \delta}{f_L - \lambda_L} + \frac{1}{\lambda_L} e^{\lambda_L \Delta_L} - \frac{1}{\lambda_L} - \frac{f_L}{f_L - \lambda_L} \Delta_L + \frac{\lambda_L}{f_L - \lambda_L} \left(\frac{\lambda_s \delta}{f_s - \lambda_s} + \frac{1}{\lambda_s} e^{\lambda_s \Delta_s} - \frac{1}{\lambda_s} - \frac{f_s}{f_s - \lambda_s} \Delta_s \right) \right\}. \tag{5}$$

From Proposition 1, it is clear that green duration in each approach is a function of the critical gaps and some other characteristics (such as discharge rate, arrival rate, and green loss) in both approaches. This demonstrates the dynamics between both approaches. When $\frac{\lambda_s}{f_s} + \frac{\lambda_L}{f_L} \to 1$, the expected green times in both approaches become infinite, which is clear by making a change to the denominator of the first term: $f_s f_L - f_s \lambda_L - f_L \lambda_s = f_s f_L \left(1 - \frac{\lambda_L}{f_L} - \frac{\lambda_s}{f_s}\right)$.

In the case of general renewal processes for vehicle arrivals, $E[t_{sa}]$ and $E[t_{La}]$ can be both obtained similarly.

The effect of the green loss δ becomes clearer when we set the critical gaps to zero (e.g. a typical queue control policy. See Kruger et al., 1990). In this case, Eqs. (4) and (5) become the following.

$$E[t_s] = \frac{\lambda_s f_L \delta}{f_s f_L - f_s \lambda_L - f_L \lambda_s} = \frac{\lambda_s \delta}{f_s \left(1 - \frac{\lambda_s}{f_s} - \frac{\lambda_L}{f_L}\right)}, \tag{6}$$

and

$$E[t_L] = \frac{\lambda_L f_s \delta}{f_s f_L - f_s \lambda_L - f_L \lambda_s} = \frac{\lambda_L \delta}{f_L\left(1-\frac{\lambda_L}{f_L}-\frac{\lambda_s}{f_s}\right)}. \tag{7}$$

Eqs. (6) and (7) give rise to the following result,

$$\frac{E[t_s]}{E[t_L]} = \frac{\lambda_s}{\lambda_L} \times \frac{f_L}{f_s}.$$

The above says the ratio of green intervals is proportionate to the ratio of vehicle arrival intensities if the discharge rates are equal in both approaches.

Then in this case, the expected duration of a full signal cycle becomes as follows.

$$C = E[t_s] + E[t_L] + \delta = \frac{\delta}{1-\frac{\lambda_L}{f_L}-\frac{\lambda_s}{f_s}}.$$

Clearly, the above property mimics that from the fixed cycle system with uniform continuum vehicle arrivals.

When the critical gap is set to zero, the following relationship becomes clear.

$$\frac{Q_s}{Q_L} = \frac{\left(1-\frac{\lambda_s}{f_s}\right)\lambda_s}{\left(1-\frac{\lambda_L}{f_L}\right)\lambda_L}, \tag{8}$$

where Q_s and Q_L are the expected queue lengths at the beginning of the green signal for the minor and major directions respectively.

When $\frac{\lambda_s}{f_s} + \frac{\lambda_L}{f_L} \to 1.0$, Eq. (8) becomes $\frac{Q_s}{Q_L} \to \frac{f_s}{f_L}$.

When the discharge rates are equal in both directions at saturated intersection, a queue clearance policy essentially ensures $Q_s = Q_L$, which is not optimal as will be seen in later tests.

2.3. Variances of green phases

Variances of green phases will be needed in the calculation of the average vehicle delay.

Variances in both approaches are inter-related. If the duration of the green phase in one approach becomes longer, expectedly the duration of the green phase in its conflict approach becomes longer as well. As a result, if the variance of the green duration in one approach becomes larger, expectedly the variance in its conflict approach becomes larger as well. The derivation in this section exploits just this observation to establish recursive equations. Note that the following derivation implies that there exist stationary variances, which is generally true at intersections that reasonably function (e.g. free of excessive vehicle queues). Be aware that the saturation flow headway of departure at the intersection is assumed constant.

Consider one vehicle at the stop line to be immediately discharged in the minor approach. Discharging this vehicle takes a constant time, D_s, where $D_s = \frac{1}{f_s}$, during which interval of time, there might be several vehicles arriving to join the queue. We denote the time for discharging this vehicle and the newly arrived ones by χ_1, and denote its probability distribution function by $P(x)$, where $P(x) = P\{\chi_1 \leqslant x\}$. If there is a queue containing i vehicles at the beginning of the green time, we denote the total time for discharging this queue by χ_i and its related distribution by $P_i(x)$ where $P_i(x) = P\{\chi_i \leqslant x\}$. Here $\chi_i = \chi_1^1 + \chi_1^2 + \ldots + \chi_1^i$, each χ_1^k is i.i.d. with χ_1. Clearly, $P_i(x)$ is an i-fold convolution of $P(x)$, which is equivalent to completely cleaning i queues of only one vehicle each at the beginning. By the theorem of total probability, the following is obvious.

$$P\{\chi_1 \leqslant x\} = \sum_{i=0}^{\infty} \frac{(\lambda_s D_s)^i}{i!} e^{-\lambda_s D_s} P\{\chi_i \leqslant x - D_s\}.$$

If we let $\Gamma(s) = E(e^{-s\chi_1})$, the Laplace-Stieltjes transform of distribution $P(x)$, then from the above analysis we have the following relationship:

$$\Gamma(s) = \sum_{i=0}^{\infty} \frac{(\lambda_s D_s)^i}{i!} e^{-\lambda_s D_s} E(e^{-s(\chi_i + D_s)}) = \exp\{D_s(\lambda_s \Gamma(s) - \lambda_s - s)\}. \tag{9}$$

The second equation uses the fact that Laplace-Stieltjes transform of $P_i(x)$ is i-th product of $\Gamma(s)$. Using the derivatives of Eq. (9) at the point where $s = 0$, we can get any moment of χ_1.

Now we can evaluate the random variable t_{sa}. Suppose that the red time t_L for the minor approach and the lost time δ, are known. During the time interval $t_L + \delta - \Delta_s$, the number of arrivals follows Poisson distribution. Therefore,

$$P\{t_{sa} \leqslant x\} = \sum_{i=0}^{\infty} \frac{(\lambda_s(t_L + \delta - \Delta_s))^i}{i!} e^{-\lambda_s(t_L + \delta - \Delta_s)} P\{\chi_i \leqslant x\}.$$

Forming the Laplace-Stieltjes transform of $P\{t_{sa} \leqslant x\}$, denoted by $F(s)$, we have the following equation:

$$F(s) = \int_0^{+\infty} e^{-sx} dP\{t_{sa} \leqslant x\} = \exp\{\lambda_s(t_L + \delta - \Delta_s)(\Gamma(s) - 1)\}. \tag{10}$$

From Eq. (9) it is easy to evaluate the first and second derivatives of $\Gamma(s)$ at $s = 0$:

$$\Gamma'(0) = -\frac{1}{f_s - \lambda_s}, \tag{11}$$

$$\Gamma''(0) = \frac{f_s}{(f_s - \lambda_s)^3}. \tag{12}$$

Hence, the expected t_{sa} conditional on $t_L + \delta - \Delta_s$ is:

$$E[t_{sa} | t_L + \delta - \Delta_s] = -F'(0) = \frac{\lambda_s(t_L + \delta - \Delta_s)}{f_s - \lambda_s}. \tag{13}$$

Eq. (13) agrees with Eq. (1) in the previous section if we take expectation of it conditional on $t_L + \delta - \Delta_s$. Eq. (13) implies a necessary condition for derivation: $\delta \geqslant \Delta_s$. A similar condition is implied later, $\delta \geqslant \Delta_L$.

The variance of t_{sa} conditional on $t_L + \delta - \Delta_s$ can be estimated as:

$$Var(t_{sa} | t_L + \delta - \Delta_s) = F''(0) - (F'(0))^2 = \frac{\lambda_s f_s (t_L + \delta - \Delta_s)}{(f_s - \lambda_s)^3}. \tag{14}$$

To obtain unconditional variances of t_{sa} and t_{La}, we need to use the relation:

$$Var(t_{sa}) = E[Var(t_{sa} | t_L + \delta - \Delta_s)] + Var(E[t_{sa} | t_L + \delta - \Delta_s]).$$

By using Eqs. (13) and (14) we have:

$$Var(t_{sa}) = \frac{\lambda_s f_s (E[t_L] + \delta - \Delta_s)}{(f_s - \lambda_s)^3} + \frac{\lambda_s^2}{(f_s - \lambda_s)^2} Var(t_L). \tag{15}$$

In previous analyses, the green time contains two periods: queue clearance time and free flow time. Because of the Markov property, these two periods are independent of each other. As a result, we have:

$$Var(t_s) = Var(t_{sa}) + Var(t_{sb}). \tag{16}$$

According to Wang (2007), $Var(t_{sb}) = -\frac{1}{\lambda_s^2} - \frac{2\Delta_s e^{\lambda_s \Delta_s}}{\lambda_s} + \frac{e^{2\lambda_s \Delta_s}}{\lambda_s^2}$. Therefore, we have the equations for variances:

$$Var(t_s) = \frac{\lambda_s f_s (E[t_L] + \delta - \Delta_s)}{(f_s - \lambda_s)^3} + \frac{\lambda_s^2}{(f_s - \lambda_s)^2} Var(t_L) - \frac{1}{\lambda_s^2} - \frac{2\Delta_s e^{\lambda_s \Delta_s}}{\lambda_s} + \frac{e^{2\lambda_s \Delta_s}}{\lambda_s^2}, \tag{17}$$

and similarly,

$$Var(t_L) = \frac{\lambda_L f_L (E[t_s] + \delta - \Delta_L)}{(f_L - \lambda_L)^3} + \frac{\lambda_L^2}{(f_L - \lambda_L)^2} Var(t_s) - \frac{1}{\lambda_L^2} - \frac{2\Delta_L e^{\lambda_L \Delta_L}}{\lambda_L} + \frac{e^{2\lambda_L \Delta_L}}{\lambda_L^2}. \tag{18}$$

It is clear now that $Var(t_s)$ and $Var(t_L)$ are linear functions of each other. Solving Eqs. (17) and (18) gives values of $Var(t_s)$ and $Var(t_L)$ as follows.

Proposition 2. *The equilibrium solutions for variances of green phases are given as follows.*

$$Var(t_s) = \left(1 - \frac{\lambda_s^2 \lambda_L^2}{(f_L - \lambda_L)^2 (f_s - \lambda_s)^2}\right)^{-1} \left(\frac{\lambda_s f_s (E[t_L] + \delta - \Delta_s)}{(f_s - \lambda_s)^3} + \frac{\lambda_s^2}{(f_s - \lambda_s)^2} \times \left[\frac{\lambda_L f_L (E[t_s] + \delta - \Delta_L)}{(f_L - \lambda_L)^3} + Var(t_{Lb})\right] + Var(t_{sb})\right), \tag{19}$$

$$Var(t_L) = \left(1 - \frac{\lambda_s^2 \lambda_L^2}{(f_L - \lambda_L)^2 (f_s - \lambda_s)^2}\right)^{-1} \left(\frac{\lambda_L f_L (E[t_s] + \delta - \Delta_L)}{(f_L - \lambda_L)^3} + \frac{\lambda_L^2}{(f_L - \lambda_L)^2} \times \left[\frac{\lambda_s f_s (E[t_L] + \delta - \Delta_s)}{(f_s - \lambda_s)^3} + Var(t_{sb})\right] + Var(t_{Lb})\right), \tag{20}$$

where $Var(t_{sb}) = -\frac{1}{\lambda_s^2} - \frac{2\Delta_s e^{\lambda_s \Delta_s}}{\lambda_s} + \frac{e^{2\lambda_s \Delta_s}}{\lambda_s^2}$ *and* $Var(t_{Lb}) = -\frac{1}{\lambda_L^2} - \frac{2\Delta_L e^{\lambda_L \Delta_L}}{\lambda_L} + \frac{e^{2\lambda_L \Delta_L}}{\lambda_L^2}$. $E[t_s]$ *and* $E[t_L]$ *are given by Eqs. (4) and (5).*

It is interesting to evaluate the green phases when the critical gap is set to zero. In this case, both $Var(t_{sb})$ and $Var(t_{Lb})$ become zero. Eqs. (19) and (20) become:

$$Var(t_s) = C_1 \left(\frac{(f_L - \lambda_L)^2 \lambda_s f_s (E[t_L] + \delta)}{(f_s - \lambda_s)} + \frac{\lambda_s^2 \lambda_L f_L (E[t_s] + \delta)}{(f_L - \lambda_L)}\right), \tag{21}$$

and

$$Var(t_L) = C_1\left(\frac{(f_s-\lambda_s)^2\lambda_L f_L(E[t_s]+\delta)}{(f_L-\lambda_L)} + \frac{\lambda_L^2\lambda_s f_s(E[t_L]+\delta)}{(f_s-\lambda_s)}\right), \tag{22}$$

where

$$C_1 = \frac{1}{\left(1-\frac{\lambda_s}{f_s}-\frac{\lambda_L}{f_L}\right)\left(f_s^2 f_L^2\left(1-\frac{\lambda_s}{f_s}-\frac{\lambda_L}{f_L}\right)+2f_s\lambda_s f_L\lambda_L\right)}. \tag{23}$$

With Eqs. (21) and (22), we can examine the impact of saturation rate on variances and intersection stability. Now we take a look at the constant C_1, represented as Eq. (23) at the right-hand sides of both Eqs. (21) and (22).

It is easily seen by Eqs. (6), (7), (21) and (22) that the expected green times and their variances increase at a rate of $O\left(\left[1-\frac{\lambda_L}{f_L}-\frac{\lambda_s}{f_s}\right]^{-1}\right)$ and $O\left(\left[1-\frac{\lambda_L}{f_L}-\frac{\lambda_s}{f_s}\right]^{-2}\right)$, respectively. Here $O(\cdot)$ is for the order of magnitude. We write $f(x) = O(g(x))$ if there exists a constant α so that $|f(x)| <= \alpha|g(x)|$. These equations indicate the critical role of green time loss in the performance of an intersection.

Proposition 3. *Given an actuated intersection with zero critical gap, both the expected values and variances of the green times increase in a linear manner with the total green time loss δ.*

As one can easily verify that with $\Delta_s = \Delta_L = 0$, symmetric intersections as a special case have $E[t_s] = E[t_L] = \frac{\lambda\delta}{f-2\lambda}$, $Var(t_s) = Var(t_L) = \frac{\lambda\delta}{(f-2\lambda)^2}$, and $\frac{\sqrt{Var(t_s)}}{E[t_s]} = \frac{\sqrt{Var(t_L)}}{E[t_L]} = \frac{1}{\sqrt{\lambda\delta}}$.

3. Vehicle delay

3.1. Vehicle delay during a signal cycle

We start with the minor approach, conditional on given t_L and δ. The waiting time has two components. When the signal first turns green in the minor approach, there has been a queue with an expected waiting time W_s^0 before the start of green time. The other component of the waiting time is incurred during the period in which the queue is being discharged. We denote this waiting time by W_{sa}. Be aware that there is no new queue during the free flow period t_{sb} as explained before. Accordingly, W_L^0 and W_{La} are the corresponding notations for the major approach.

Proposition 4. *At the time when the green light first turns on in the minor approach, the total vehicle delay, denoted by W_s^0, of those arrivals N_s, during the red signal period is given as follows.*

$$E[W_s^0] = \frac{1}{2}\lambda_s(Var(t_L) + E^2[t_L] + 2(\delta-\Delta_s)E[t_L] + (\delta-\Delta_s)^2), \tag{24}$$

and similarly for the major approach,

$$E[W_L^0] = \frac{1}{2}\lambda_L(Var(t_s) + E^2[t_s] + 2(\delta-\Delta_L)E[t_s] + (\delta-\Delta_L)^2). \tag{25}$$

Proof. According to Ross (1997), with a given number of arrivals from a Poisson process during a time period, the distribution of each arrival is uniform within the given time interval. Therefore, the expected waiting time of the queue can be calculated by conditioning on the length of queue as follows.

$$\begin{aligned}
E[W_s^0] &= E[E[E[E[W_s^0|X(t_L+\delta-\Delta_s)]]|t_L]] \\
&= E[(t_L+\delta-\Delta_s)\times\lambda_s\times\tfrac{1}{2}\times(t_L+\delta-\Delta_s)] \\
&= \tfrac{1}{2}\lambda_s E[(t_L+\delta-\Delta_s)^2] \\
&= \tfrac{1}{2}\lambda_s(E[t_L^2] + 2(\delta-\Delta_s)E[t_L] + (\delta-\Delta_s)^2) \\
&= \tfrac{1}{2}\lambda_s(Var(t_L) + E^2[t_L] + 2(\delta-\Delta_s)E[t_L] + (\delta-\Delta_s)^2).
\end{aligned}$$

Similarly, we can show the result for $E[W_L^0]$. □

We further have the following results for W_{sa} and W_{La}, respectively.

Proposition 5. *The waiting times during queue discharge are given as follows.*

$$E[W_{sa}] = \frac{1}{2}(f_s-\lambda_s)(Var(t_{sa}) + E^2[t_{sa}]), \tag{26}$$

and similarly,

$$E[W_{La}] = \frac{1}{2}(f_L - \lambda_L)(Var(t_{La}) + E^2[t_{La}]). \tag{27}$$

Proof. We only prove for the minor approach. The result for the major approach can be obtained similarly.

We condition on queue discharge time t_{sa}.

$$\begin{aligned} E[W_{sa}|t_{sa}] &= E[\int_0^{t_{sa}} [X(t_L + \delta - \Delta_s) + X(t) - f_s t]dt|t_{sa}] \\ &= E[\int_0^{t_{sa}} X(t_L + \delta - \Delta_s)dt|t_{sa}] + E[\int_0^{t_{sa}} (\lambda_s t - f_s t)dt|t_{sa}] \\ &= (f_s - \lambda_s)t_{sa}^2 + \tfrac{1}{2}(\lambda_s - f_s)t_{sa}^2 \\ &= \tfrac{1}{2}(f_s - \lambda_s)t_{sa}^2. \end{aligned}$$

The third equality above uses the fact that $E[X(t_L + \delta - \Delta_s)|t_{sa}] = (f_s - \lambda_s)t_{sa}$ according to Eq. (1).

We therefore have,

$$E[W_{sa}] = E[E[W_{sa}|t_{sa}]] = \frac{1}{2}(f_s - \lambda_s)(Var(t_{sa}) + E^2[t_{sa}]). \qquad \square$$

To summarize, the total expected vehicle delay during the period of a signal cycle at the intersection can be expressed in a closed form by $E[W_s^0] + E[W_L^0] + E[W_{sa}] + E[W_{La}]$ explicitly. We can calculate the expected waiting time by substituting the equations for the expected values and variances.

3.2. Vehicle delay per unit time

The signal cycling can be considered as a renewal process, from the beginning of a green time to the beginning of the green time again. According to the renewal theory, the average vehicle delay per unit time over this renewal process is the ratio between the total expected vehicle delay in a cycle and the expected cycle length. This average vehicle delay can therefore be expressed in terms of Δ_s and Δ_L with given parameters λ_s, λ_L, f_s and f_L. We denote by $F(\Delta_L, \Delta_s)$ the function of average vehicle delay per unit time. The function $F(\Delta_L, \Delta_s)$ can be expressed in the following way.

$$F(\Delta_L, \Delta_s) = \frac{E[W_s^0] + E[W_L^0] + E[W_{sa}] + E[W_{La}]}{E[t_s] + E[t_L] + \delta}. \tag{28}$$

Similarly, one can easily get directional average waiting time per vehicle or per time unit, which we do not pursue in details here.

The closed form (28) of $F(\Delta_L, \Delta_s)$ consists of a large number of terms, making it very inconvenient to analytically examine its properties such as concavity or convexity. However, our observation is that the delay function appears to be a coercive function in the critical gap. This means that as the critical gap increases, the delay increases and tends to infinity. We can easily study this function numerically with latest computing technologies.

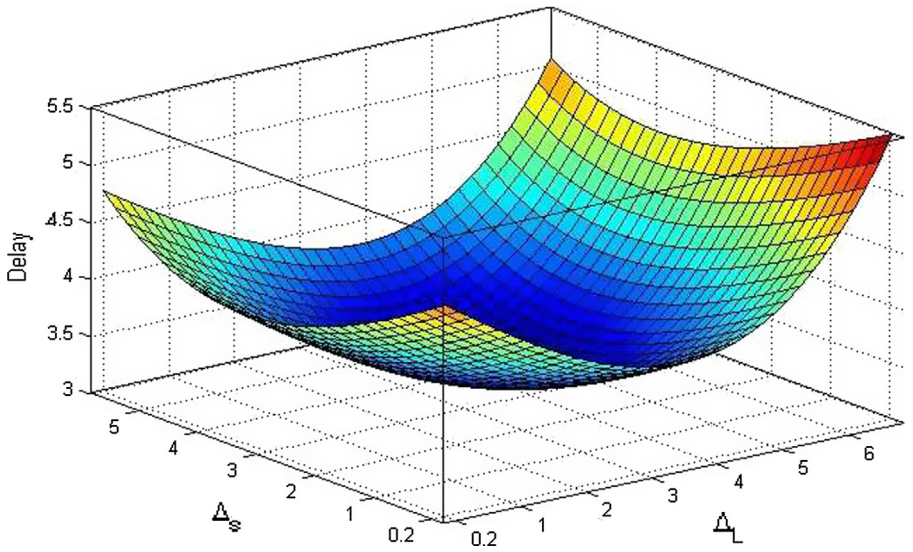

Fig. 4. Example average delay per unit time with $\delta = 6.0$, $\lambda_s = 0.20$ and $\lambda_L = 0.25$.

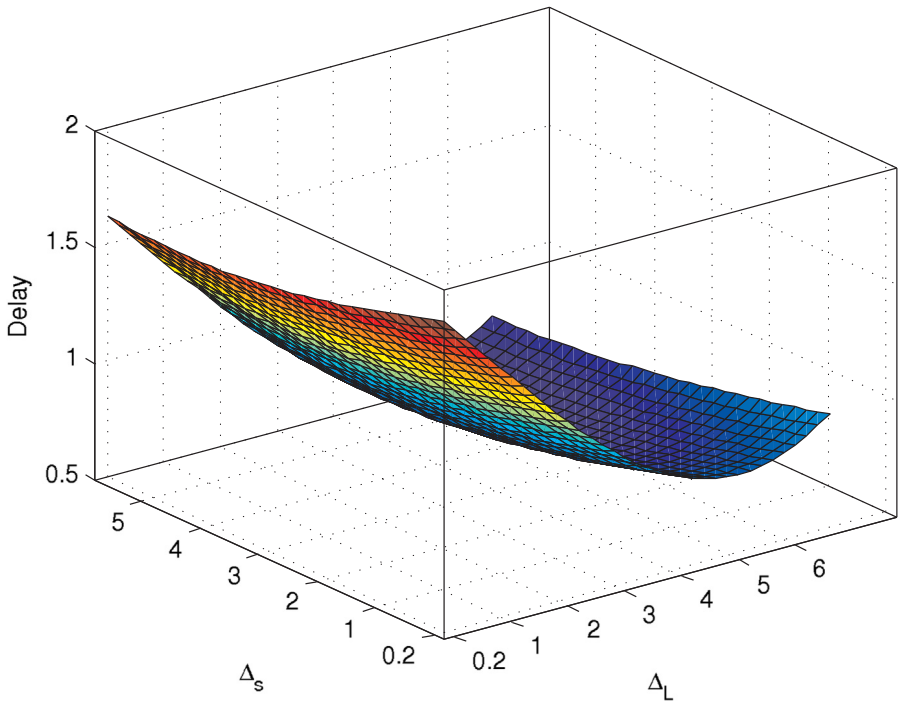

Fig. 5. Example average delay per unit time $\delta = 6.0$, $\lambda_s = 0.05$ and $\lambda_L = 0.25$.

Fig. 4 graphically demonstrates an example delay function when $\delta = 6.0$, $\lambda_s = 0.20$, $\lambda_L = 0.25$, $f_s = 0.6$ and $f_L = 0.6$. The optimal delay is 3.157 vehicle seconds at $\Delta_s = 3.4s$ and $\Delta_L = 3.6s$.

In addition, we examined a case as illustrated in Fig. 5, in which the discharge rates in both approaches are 0.6 and 0.4 vehicle per second, respectively. The arrival rates are 0.05 and 0.25 vehicles per second, respectively. The green loss during a cycle is 6 s. The average vehicle delay reaches its minimum when $\Delta_s = 5.2$ and $\Delta_L = 5.2$ seconds. Intuitively, the close proximity of the critical gaps is surprising as one would intuitively think the critical gap for the minor direction should be much smaller than that for the major direction.

Now we are able to evaluate intersection performance in various settings. Table 1 is a sample test result where $f_s = f_L = 0.6$ vehicle per second and Table 2 is with $f_s = 0.4$ and $f_L = 0.6$ vehicle per second.

From Table 1, we have the following observations.

Observation 1. When roadway capacities are comparable between the two approaches, the optimal green extensions in both directions are almost equivalent regardless of traffic intensities, with the major direction having a slightly larger extension.

Table 1 is for an intersection with symmetric discharging capacities for both approaches as compared to Table 2, whose discharging capacities of both approaches are significantly disparate. Both Tables 1 and 2 show smaller optimal critical gap as traffic increase at the intersection, which is intuitive because a larger traffic means a longer queue at conflicting approaches and harder to extend green time at the current approach. In other words, when expectedly a longer queue is already present at conflicting approaches, it is likely optimal to adopt a smaller critical gap for free flow at the current approach.

3.3. Numerical results about queue clearance policy

The often mentioned queue clearance policy in literature entails signal switch if and only if the queue is cleared in the current approach. It corresponds to setting both critical gaps to zero in our study here, e.g. $\Delta_L = \Delta_s = 0.0$. Our study enables us to compare

Table 1
Optimal critical gap and intersection performance with $f_s = f_L = 0.6$, $\delta = 4.0$.

λ_s/λ_L	Δ_s/Δ_L	$E[t_s]$	$E[t_L]$	$Var(t_s)$	$Var(t_L)$	$F(\cdot,\cdot)$
0.05/0.25	3.8/4.4	0.76	3.87	2.1	24.9	0.234
0.08/0.25	3.6/4.2	1.24	3.97	3.7	24.2	0.441
0.10/0.25	3.6/4.0	1.62	4.02	5.3	23.6	0.603
0.15/0.25	3.4/3.6	2.73	4.47	11.3	26.7	1.142
0.20/0.25	3.2/3.4	4.47	5.58	25.9	38.9	2.029

Table 2
Optimal critical gap and intersection performance with $f_s = 0.4, f_L = 0.6, \delta = 6.0$.

λ_s/λ_L	Δ_s/Δ_L	$E[t_s]$	$E[t_L]$	$Var(t_s)$	$Var(t_L)$	$F(\cdot,\cdot)$
0.05/0.25	5.2/5.2	1.91	7.41	8.1	60.4	0.607
0.08/0.25	4.8/4.6	3.18	7.30	15.9	51.5	1.105
0.10/0.25	4.6/4.4	4.32	7.84	25.1	56.2	1.543
0.15/0.25	4.4/3.6	9.04	10.40	88.8	95.3	3.481
0.20/0.25	4.2/2.8	27.03	22.84	751.0	492.7	11.095

Table 3
Queue clearance performance with $f_s = f_L = 0.6, \delta = 4.0$.

λ_s/λ_L	$F(\cdot,\cdot)$
0.05/0.25	1.27
0.08/0.25	1.56
0.10/0.25	1.80
0.15/0.25	2.55
0.20/0.25	3.73

Table 4
Queue clearance performance with $f_s = 0.4, f_L = 0.6, \delta = 6.0$.

λ_s/λ_L	$F(\cdot,\cdot)$
0.05/0.25	1.83
0.08/0.25	2.45
0.10/0.25	2.99
0.15/0.25	5.41
0.20/0.25	14.66

the intersection performance between the queue clearance policy as in Table 3 and 4 as opposed to the performance in Tables 1 and 2 respectively. The last entries of Table 3 and Table 4 have a $\frac{V}{C} = 0.75$ and 0.92 respectively, both considered as heavy traffic. The queue clearance policy shows a significantly larger vehicle delay as compared to the optimally set actuated control.

4. The case of general traffic

Our primary concern is intersection performance with general stationary arriving traffic under an actuated signal system. In this case, we assume that vehicle arrivals follow a general renewal process. In this renewal process, vehicle headways are independent and identically distributed (*i.i.d.*) random variables whose density function is denoted by $f(\cdot)$. The arrival intensity is λ, and we use H for the stochastic arrival headway. Clearly, we have $\lambda E[H] = 1$. We use σ^2 for the variance of H, and the subscripts L and s denote the major and minor directions, respectively. In the following, notations without subscriptions indicate results applicable to both directions. We will develop analytical results following the framework earlier.

First, we characterize the free flow green time with general vehicle headway. The notation has the same meaning as in the previous sections. Derivation of the results is seen in Wang et al. (2010).

$$E[t_{sb}] = \frac{\int_0^{\Delta_s} tf(t)dt}{1-F(\Delta_s)}, \tag{29}$$

$$E[t_{Lb}] = \frac{\int_0^{\Delta_L} tf(t)dt}{1-F(\Delta_L)}, \tag{30}$$

$$Var(t_{sb}) = \frac{\int_0^{\Delta_s} t^2 f(t)dt}{1-F(\Delta_s)} + E^2[t_{sb}], \tag{31}$$

$$Var(t_{Lb}) = \frac{\int_0^{\Delta_L} t^2 f(t)dt}{1-F(\Delta_L)} + E^2[t_{Lb}]. \tag{32}$$

4.1. Expectations

Following similar steps as in the Poisson process using the results (29)–(32), we have the following accordingly.

Proposition 6. *For the general traffic, the expected lengths of green phases are given as follows.*

$$E[t_s] = \frac{(f_s-\lambda_s)(f_L-\lambda_L)}{f_sf_L-f_s\lambda_L-f_L\lambda_s} \times \left\{ \frac{\lambda_s\delta}{f_s-\lambda_s} + \frac{\int_0^{\Delta_s} tf(t)dt}{1-F(\Delta_s)} - \frac{\lambda_s}{f_s-\lambda_s}\Delta_s + \frac{\lambda_s}{f_s-\lambda_s}\left(\frac{\lambda_L\delta}{f_L-\lambda_L} + \frac{\int_0^{\Delta_L} tf(t)dt}{1-F(\Delta_L)} - \frac{\lambda_L}{\lambda_L-\lambda_L}\Delta_L \right) \right\}, \tag{33}$$

$$E[t_L] = \frac{(f_s-\lambda_s)(f_L-\lambda_L)}{f_sf_L-f_s\lambda_L-f_L\lambda_s} \times \left\{ \frac{\lambda_L\delta}{f_L-\lambda_L} + \frac{\int_0^{\Delta_L} tf(t)dt}{1-F(\Delta_L)} - \frac{\lambda_L}{f_L-\lambda_L}\Delta_L + \frac{\lambda_L}{f_L-\lambda_L}\left(\frac{\lambda_s\delta}{f_s-\lambda_s} + \frac{\int_0^{\Delta_s} tf(t)dt}{1-F(\Delta_s)} - \frac{\lambda_s}{f_s-\lambda_s}\Delta_s \right) \right\}. \tag{34}$$

Discretization of the integral for any known probability density function $f(\cdot)$ above easily gives rise to its numerical solution.

4.2. Some prerequisite results

The following results are needed for the subsequent derivations of variances and waiting time.

Theorem 1. *Given a constant t, the following holds for both directions under heavy traffic:*

$$E[X(t)] \approx \lambda t, \tag{35}$$

$$Var(X(t)) \approx kt, \tag{36}$$

where $k = \frac{\sigma^2}{E^3[H]}$.

Here H is the random variable for vehicle headway and σ^2 is the variance of H. In the special case of Poisson arrivals (e.g., headway with exponential distribution), we can easily verify that $k = \lambda$, in which case values in Theorem 1 are accurate. In general cases of heavy traffic where vehicle headway is small compared to the green time in each direction, Theorem 1 provides good approximations. One way of its proof is indicated in Grimmett and Stirzaker (2001), which states that for a renewal process, the mean and variance of number of arrivals follow the Central Limit Theorem during a large time period.

The following result about waiting time corresponds to Proposition 4.

Proposition 7. *Under heavy traffic, the expected vehicle waiting time $w(t)$ is approximately $\frac{\lambda t^2}{2}$, i.e., $w(t) \approx \frac{\lambda t^2}{2}$, where t is the time that the signal has been red in the direction of interest, assuming no queue present at the beginning of the red time.*

The proof is provided in Appendix A.

4.3. Variances

In previous analysis, we use χ_1 to denote the time needed for reducing the vehicle queue length by one vehicle. Because the vehicles having arrived during the red time are $X(t_L+\delta)$ for the minor approach, the total time for discharging these vehicles is equal to $\sum_{i=1}^{X(t_L+\delta-\Delta_s)} \chi_1^i$, where χ_1^i is i.i.d. with χ_1. Therefore, using $Var(t_{sa}) = E[Var(t_{sa}|X(t_L+\delta-\Delta_s))] + Var(E[(t_{sa}|X(t_L+\delta-\Delta_s)])$, we have:

$$\begin{aligned} Var(t_{sa}) &= E\left[\sum_{i=1}^{X(t_L+\delta-\Delta_s)} Var(\chi_1^i)|X(t_L+\delta-\Delta_s) \right] + Var\left(\sum_{i=1}^{X(t_L+\delta-\Delta_s)} E[\chi_1^i]|X(t_L+\delta-\Delta_s) \right) \\ &= Var(\chi_1)E[X(t_L+\delta-\Delta_s)] + (E[\chi_1])^2 Var(X(t_L+\delta-\Delta_s)) \\ &= \lambda_s Var(\chi_1)(E[t_L]+\delta-\Delta_s) + (E[\chi_1])^2(k(E[t_L]+\delta-\Delta_s) + \lambda_s^2 Var(t_L)). \end{aligned}$$

Similarly, we can evaluate $Var(t_{La})$ as follows

$$Var(t_L) = \lambda_L Var(\mu_1)(E[t_s]+\delta-\Delta_L) + (E[\mu_1])^2(k(E[t_s]+\delta-\Delta_L) + \lambda_L^2 Var(t_s)).$$

where μ_1 is the counterpart definition of χ_1 for the major road, which is the time for reducing the queue length by one vehicle. When the arrivals follow Poisson distribution, the equation for $Var(t_{sa})$ becomes Eq. (14). Recall that $Var(t_s) = Var(t_{sa}) + Var(t_{sb})$. The following results become obvious.

Proposition 8. *The variances of green phases are given as follows for the minor and major roads respectively.*

$$Var(t_s) = \lambda_s Var(\chi_1)(E[t_L] + \delta - \Delta_s) + (E[\chi_1])^2(k(E[t_L] + \delta - \Delta_s) + \lambda_s^2 Var(t_L)) + Var(t_{sb}), \tag{37}$$

$$Var(t_L) = \lambda_L Var(\mu_1)(E[t_s] + \delta - \Delta_L) + (E[\mu_1])^2(k(E[t_s] + \delta - \Delta_L) + \lambda_L^2 Var(t_s)) + Var(t_{Lb}), \tag{38}$$

where $E[\chi_1]$ *and* $Var(\chi_1)$ *are given by the following equations as from the earlier results.*

$$E[\chi_1] = \frac{1}{f_s - \lambda_s},$$
$$Var[\chi_1] = \frac{f_s}{(f_s - \lambda_s)^3} - \frac{1}{(f_s - \lambda_s)^2} = \frac{\lambda_s}{(f_s - \lambda_s)^3},$$
$$E[\mu_1] = \frac{1}{f_L - \lambda_L},$$
$$Var[\mu_1] = \frac{f_L}{(f_L - \lambda_L)^3} - \frac{1}{(f_L - \lambda_L)^2} = \frac{\lambda_L}{(f_L - \lambda_s)^3}.$$

The last four formulas in Proposition 8 are borrowed from those on Poisson assumptions. Note that Proposition 4 about waiting time provides asymptotic approximations in heavy traffic according to Proposition 7 and Theorem 1. Proposition 5 also holds in heavy traffic due to Theorem 1. For the according values in general traffic, we only need to update the variances and expected values of green times in Propositions 4 and 5 with their according values from Propositions 6 and 8. Using Eq. (28), we can estimate the average vehicle delay under heavy traffic.

Note that the results here about green time variance, waiting time and average vehicle waiting time are all asymptotically accurate under heavy traffic. The numerical tests next show that the formulas perform well in evaluating the intersection performance.

4.4. Numerical results in heavy traffic

In generating arriving traffic for the numerical tests, we assume the headway follows Gamma distribution.

$$f(x) = \frac{\exp(-x/\theta)}{\Gamma(k)\theta^k} x^{k-1},$$

where the mean is $\theta k = \lambda_s$ (for minor direction) or λ_L (for major direction). The parameter k is given by the coefficient of variation (CV) in the following tests. The same CV value applies to both directions each time. For each case, we simulate 120 times Monte Carlo

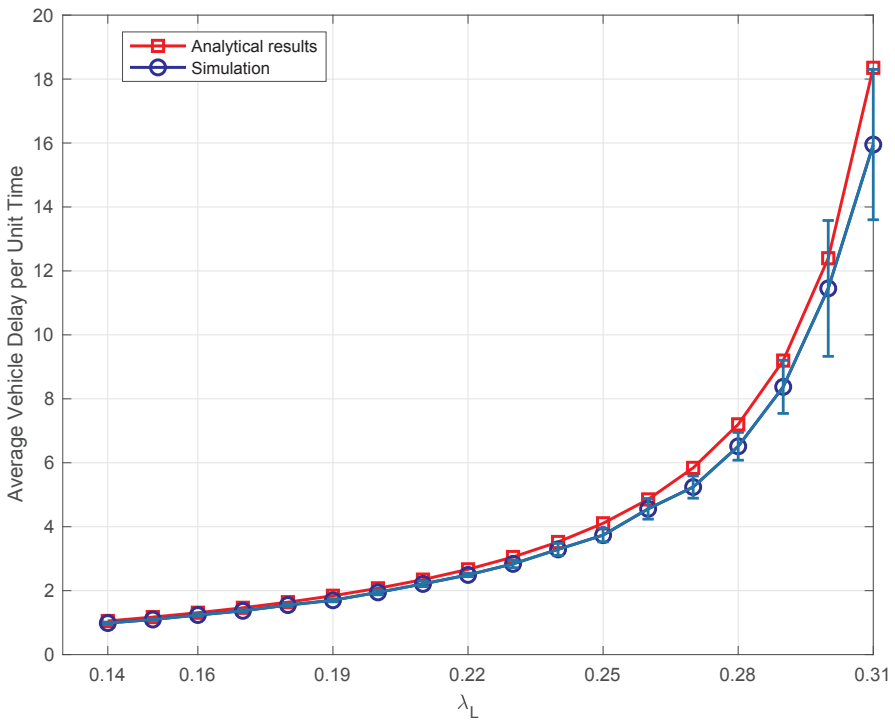

Fig. 6. $f_s = 0.6$, $\lambda_s = 0.2$, $f_L = 0.5$, $CV = 0.5774$.

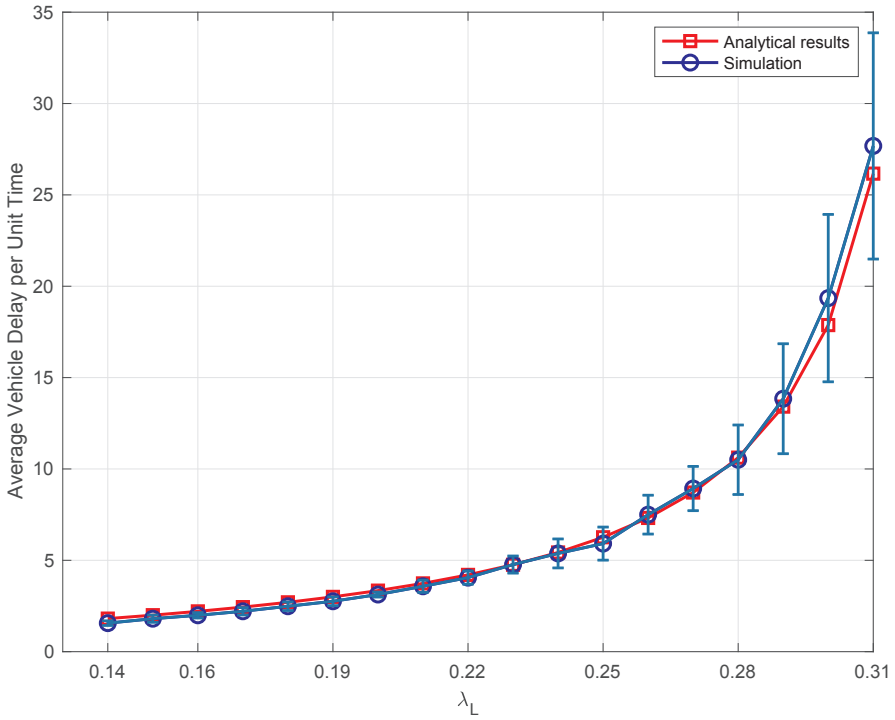

Fig. 7. $f_s = 0.6$, $\lambda_s = 0.2$, $f_L = 0.5$, $CV = 1.4142$.

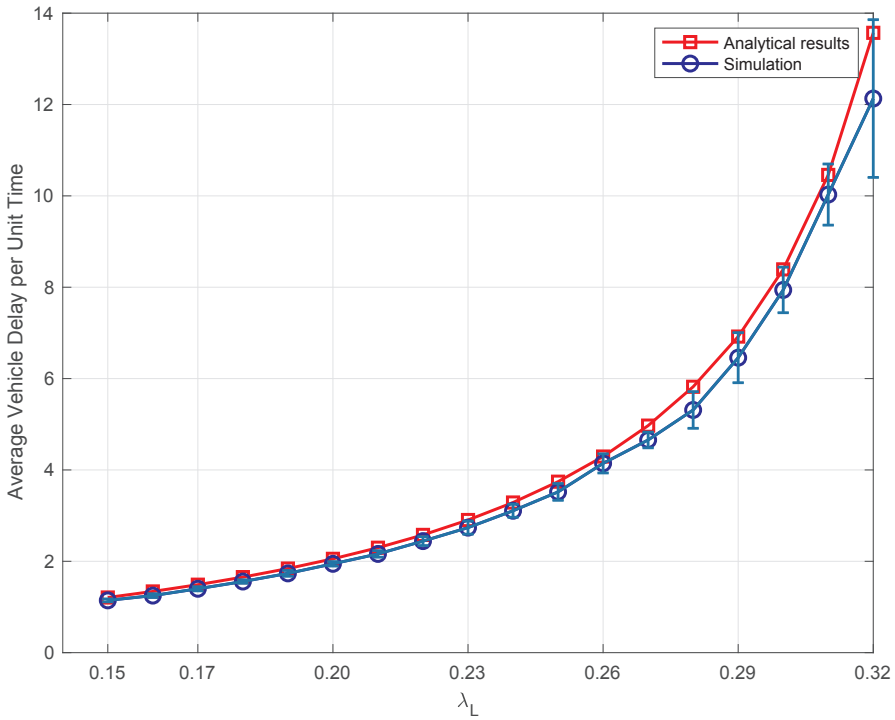

Fig. 8. $f_s = 0.5$, $\lambda_s = 0.2$, $f_L = 0.6$, $\Delta_s = 3.5$, $\Delta_L = 3.5$, $CV = 0.5774$.

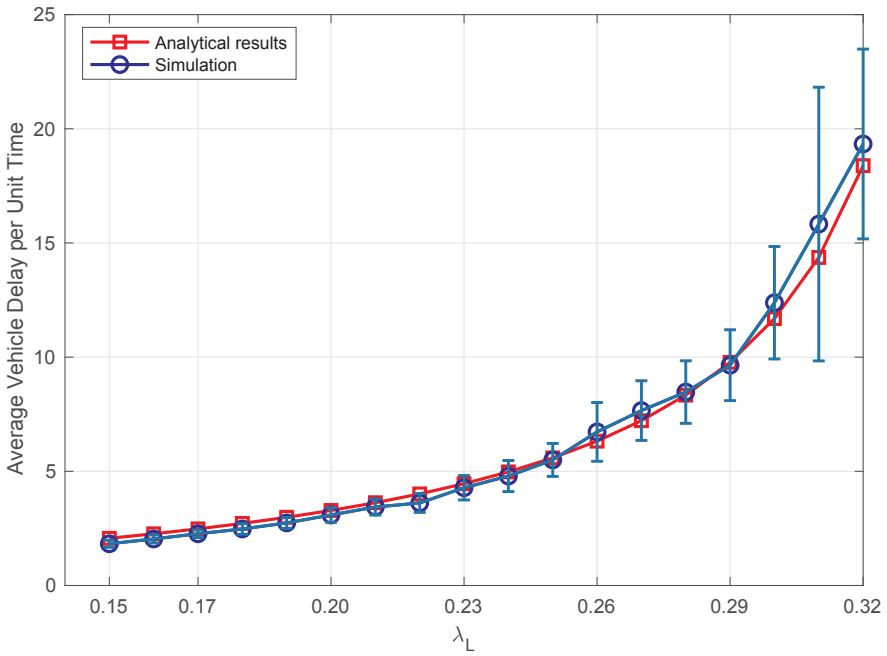

Fig. 9. $f_s = 0.5$, $\lambda_s = 0.2$, $f_L = 0.6$, $\Delta_s = 3.5$, $\Delta_L = 3.5$, $CV = 1.4142$.

simulation. In each time, we guarantee no less than 4000 arriving vehicles in each direction, which turns out to be at least 120 signal cycles. All other parameters in the simulation are set as in the analytical formulas such as discharge rates.

In Figs. 6 and 7, $\lambda_s = 0.2, f_s = 0.6, f_L = 0.5, \delta = 6.0, \Delta_s = 3.5, \Delta_L = 3.2$. We vary λ_L from 0.14 to 0.31, i.e., $\frac{\lambda_L}{f_L} + \frac{\lambda_s}{f_s} \in [0.6133, 0.9533]$. The only difference between Figs. 6 and 7 is the value of *CV*. In Fig. 6, the CV is 0.5774 while in Fig. 7, the CV is 1.4142. In these two figures, the blue error bar (e.g. vertical blue bar) represents one standard deviation of simulated results above and blow the average (e.g. blue curve) value respectively.

We change the setting for f_s and f_L in Figs. 8 and 9, where $\lambda_s = 0.20, f_s = 0.5, f_L = 0.6, \delta = 6.0, \Delta_s = 3.5, \Delta_L = 3.5$. We vary λ_L from 0.15 to 0.32, which yields $\frac{\lambda_L}{f_L} + \frac{\lambda_s}{f_s} \in [0.6500, 0.9333]$. In Fig. 8, the *CV* is 0.5744. In Fig. 9, the *CV* is 1.4142. As an example of green time variation, the average green time is 30 and the standard deviation becomes 32 in the case above in which $\lambda_s = 0.20$ and $\lambda_L = 0.31$.

The analytical results for heavy traffic are exact in the case of Poisson distributed headway. Fig. 10 shows analytical results with Poisson arrivals compared with those from simulation, other parameters identical to those in Figs. 8 and 9. The slight disagreement between the analytical and simulation due to variations in simulation explains the quality of the performances in Figs. 6–9. Obviously, by comparing Fig. 6 with 7 and Fig. 8 with 9, the analytical estimate of waiting time appears better when the CV of the arrival headway is larger.– A larger CV of arrival headway means larger variation of vehicle arrivals. By information, we have examined the vehicle headway for arriving traffic based on the loop detector information at an intersection in the City of Minneapolis in Minnesota. The data shows a CV of headway ranging from 1.2 to 1.9 during day time. This information supports our numerical tests of the models for general traffic, and appears that the findings from the numerical test therein are valid.

The above figures also indicate very large variances of green times under very heavy traffic.

5. Conclusion and further discussions

This research studies a vehicle-actuated signal control scheme in which the critical gap is the only control variable. We analytically model the intersection performance in two cases respectively: Poisson arrivals and general traffic. Equations for expected green times in both directions, variances, and the average waiting time are presented. The models in the case of Poisson processes are exact. The models in the case of heavy traffic are generally accurate, but appear sensitive to the variance of headway. The models can be used for studying setup of critical gaps and for example performance evaluation.

Our models illustrate some similarities between the actuated signal system and the pre-timed one. The latter best serves a uniform vehicle arrival. It has the same green time allocation as the expected green time allocation in an actuated signal system when the critical gap is set to zero.

One insight from our modeling is that average vehicle delay appears a coercive function with the critical gaps and that the optimal critical gaps are generally not zero. This indicates that the queue clearance policy even in heavy traffic is likely not optimal. However, the findings here could change if the number of queuing vehicles in the subsequent phases is used as a condition for signal switch. In other words, the actuated signal control, which does not consider subsequent phase queueing, is an adaptive but rather limited

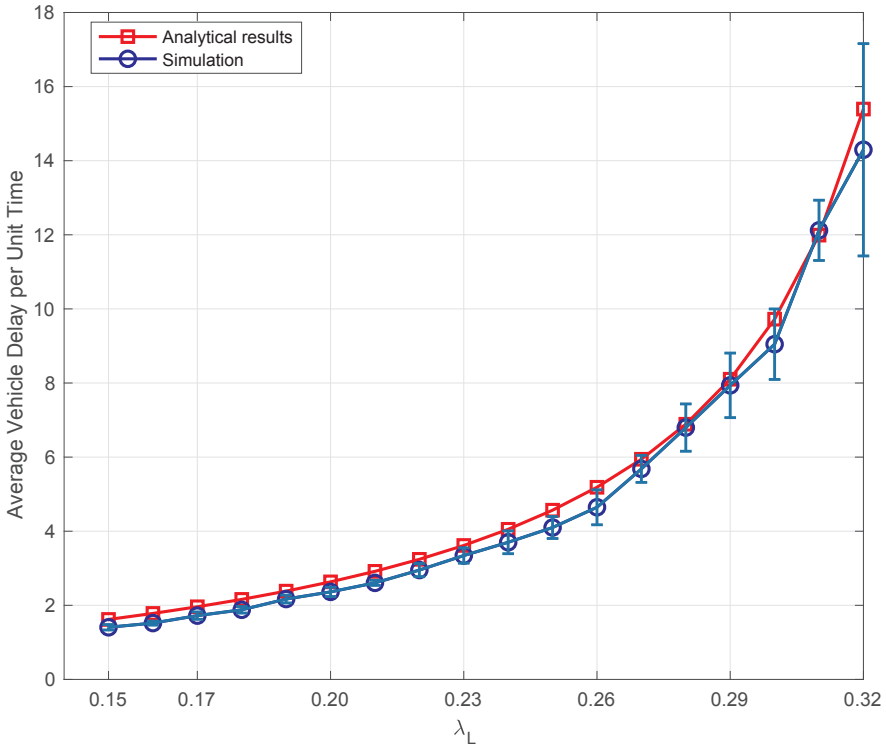

Fig. 10. $f_s = 0.5$, $\lambda_s = 0.2$, $f_L = 0.6$, $\Delta_s = 3.5$, $\Delta_L = 3.5$, Poisson headway.

scheme (Wang et al., 2017). Nevertheless, its ease of application has greatly contributed to its popularity in practice.

Regarding the fully actuated signal control, our numerical tests on one hand confirm that heavier traffic generally justify smaller critical gaps as in Tables 1 and 2. On the other hand, however, Tables 1 and 2 also indicate optimal critical gaps that counter many people's presumption which often presumes a much smaller critical gap for the minor approach. According to Tables 1 and 2, the minor approach has a slightly smaller optimal critical gap but by a trivial margin. Our interpretation is that the critical gap of an approach affects vehicle delay for *all* the approaches because of the dynamic interactions between phases, which is often overlooked or underestimated in many people's presumption. This dynamic effect may only be captured by models that explicitly consider the interaction of phases. Our numerical tests also show that the optimal critical gaps may be up to 4 or 5 s as compared to the typical value of only 2 s in practice.

Results in this paper rely on an assumption of a steady state arrival process of vehicles, which does not agree well with the phenomenon of platoon arrivals. In addition, the assumption of no maximum/minimum green times ignores the overflow (e.g. residual) queues from the prior cycle when a maximum green is enforced. Although these (rather strong) assumptions have enabled the authors to develop the analytical results, it would still be interesting to explore relaxation of some or all of them in the future. But the authors believe the big picture revealed in this paper would still generally hold true.

Acknowledgement

This paper is partially the second author's Ph.D. dissertation. A grant from the Southwest Regional University Transportation Center (SWUTC) partially supported this research.

Appendix A

A.1. Proof of Proposition 7

We have

$$w(t) = \int_0^t (t-l + w(t-l))f(l)dl.$$

The above equation conditions on the first vehicle arrival at time l from the beginning of the red time. We only need to see if the assumption can approximately satisfy the above equation.

Left handside=$\frac{1}{2}\lambda t^2$.

Right handside=$t-E[H]+\int_0^t \frac{1}{2}\lambda(t-l)^2 f(l)dl$

$$= t-E[H]+\frac{1}{2}\lambda(t^2-2tE[H]+\sigma^2+E^2[H])$$

$$\approx \frac{1}{2}\lambda t^2+\frac{1}{2}\lambda\sigma^2-\frac{1}{2}E[H].$$

Note that $\int_0^t (t-l)f(l)dl \approx t-E[H]$ when there are a few cars during the red time t each time, implying a big enough t relative to the average headway. We call the remnant in the right hand side $\frac{1}{2}\lambda\sigma^2-\frac{1}{2}E[H]$ error term. The assumption can make both sides of the equation approximately equal, considering t outweighs $E[H]$ and t^2 outweighs σ^2. In the following, we show how t^2 outweighs σ^2.

$$\frac{1}{2}\lambda\sigma^2 = \frac{1}{2}\lambda v E[H]\sigma$$

$$= \frac{1}{2}v\sigma$$

$$= \frac{1}{2}v^2 E[H],$$

where v is the coefficient of variation (CV) between the standard deviation σ and the expected headway $E[H]$. If CV is a finite value, then the error compared with the major term $\frac{1}{2}\lambda t^2$ tends to zero in heavy traffic. In Poisson arrivals as a special case, the error term is zero, which can be verified by interested readers. □

References

Akçelik, R., 1981. Traffic Signals: Capacity and Timing Analysis. Technical report. ARR No.123. Australian Road Research Board, Nunawading, Australia.

Akçelik, R., 1994. Estimation of green times and cycle time for vehicle-actuated signals. Transp. Res. Rec. 1457, 63–72.

Akçelik, R., Rouphail, N.M., 1993. Estimation of delays at traffic signals for variable demand conditions. Transp. Res. B: Methodol. 27 (2), 109–131.

Akçelik, R., Chung, E., Besley. M., 1997. Recent research on actuated signal timing and performance evaluation and its application in SIDRA5. Technical report. In: the Compendium of Technical Papers of the 67th Annual Meeting of the Institution of Transportation Engineers, Boston, USA.

Bonneson, J.A., Mccoy, P.T., 1995. Average duration and performance of actuated signal phases. Transp. Res. Part A: Policy Pract. 29 (6), 429–443.

Courage, K., Fambro, D., Akcelik, R., Lin, P.-S., Anwar, M., Viloria, F., 1996. Capacity analysis of traffic actuated intersections. Technical report. NCHRP Project 3-48 Final Report Prepared for National Cooperative Highway Research Program, Transportation Research Board, National Research Council.

Cowan, R., 1978. An improved model for signalised intersections with vehicle-actuated control. J. Appl. Probab. 15 (2), 384–396.

Daniel, J., Fambro, D.B., Rouphail, N.M., 1996. Accounting for nonrandom arrivals in estimate of delay at signalized intersections. Transp. Res. Rec. 1555, 9–16.

Darroch, J.N., Newell, G.F., Morris, R.W.J., 1964. Queues for a vehicle-actuated traffic light. Oper. Res. 12 (6), 882–895.

Federal Highway Administration. 2004. Some Statistics of ITS Depoyment Administratered by the Research and Innovative Technology Administation (RITA). < http://www.itsdeployment.its.dot.gov > (last Accessed March 20, 2013).

Grimmett, G., Stirzaker, D., 2001. Probability and Random Processes, third ed. Oxford University Press Inc., New York, pp. 417 (Chapter 10.2).

Hawkes, A.G. 1963. Queuing at traffic intersections. In: Almond, L. (Ed.), Proceedings of the Second International Symposium on the Theory of Road Traffic Flow, London, 1963. OECD, Paris, 1965, pp. 190–199.

Kimber, R., Hollis, E., 1979. Traffic Queues and Delay at Road Junctions. Technical Report. TRRL Laboratory Report No. 909. Transport and Road Research Laboratory, Berkshire, U.K.

Kruger, P., May, A.D., Newell, G.F., 1990. The Efficient Control of an Isolated Vehicle-Actuated Controlled Intersection: A Comparison between Queue Control and Volume-Density Control. Research Report, UCB-ITS-RR-90-1. Institute of Transportation Studies, University of California at Berkeley.

Lehoczky, J.P., 1972. Traffic intersection control and zero-switch queues. J. Appl. Probab. 9 (2), 382–395.

Li, J., Rouphail, N.M., Akçelik, R., 1994. Overflow delay estimation for a simple intersection with fully actuated signal control. Transp. Res. Rec. 1457, 73–81.

Li, J., Rouphail, N.M., Tarko, A., Velichansky, L., 1996. Overflow delay model for signalized arterials. Transp. Res. Rec. 1555, 1–8.

Lin, F.-B., 1982a. Estimation of average phase durations for full-actuated signals. Transp. Res. Rec. 881, 65–72.

Lin, F.-B., 1982b. Predictive models of traffic actuated cycle splits. Transp. Res. Part B: Methodol. 16 (5), 361–372.

Lin, P.-S., Courage, K.G., 1996. Phase time prediction for traffic-actuated intersections. Transp. Res. Rec. 1555, 17–22.

Mirchandani, P.B., Ning, Z., 2007. Queuing models for analysis of traffic adaptive signal control. IEEE Trans. Intell. Transp. Syst. 8 (1), 50–59.

Malakapalli, M., Messer, C.J., 1993. Enhancements to the PASSER II-90 delay estimation procedures. Transp. Res. Rec. 1421, 94–103.

Newell, G.F., 1969. Properties of Vehicle-actuated Signals: I. One-way streets. Transp. Sci. 3 (1), 30–52.

Rouphail, N., Anwar, M., Fambro, D., Sloup, P., Perez, C., 1997. Validations of generalized delay model for vehicle-actuated traffic signals. Transp. Res. Rec. 1572, 105–111.

Ross, S.M., 1997. Introduction to Probability Models, 6th ed. Academic Press (Chapter 4).

Tanner, J.P., 1953. A problem of interference between two queues. Biometrika 40 (1–2), 58–69.

Viti, F., Van Zuylen, H.J., 2010. A probabilistic model for traffic at actuated control signals. Transp. Res. Part C: Emerg. Technol. 18 (3), 299–310.

Wang, X., 2007. Modeling the process of information relay through inter-vehicle communication. Transp. Res. Part B: Methodol. 41 (6), 684–700.

Wang, X., Cao, X., Wang, C., 2017. Dynamic optimal real-time algorithm for signals (DORAS): case of isolated roadway intersections. Transp. Res. Part B: Methodol. 106, 433–446.

Wang, X., Adams, T.M., Jin, W.-L., Meng, Q., 2010. The process of information propagation in a traffic stream with a general vehicle headway: a revisit. Transp. Res. Part C: Emerg. Technol. 18 (3), 367–375.

Webster, F.V. 1958. Traffic Signal Settings. Technical report. Road Research Technical Paper No. 39. Department of Scientific and Industrial Research, Road Research Laboratory, HMSO, London, U.K.